Cavity effect on a biexciton in a CuCl microcavity

Yasuyoshi Mitsumori,[1,*] Shimpei Matsuura,[1] Shoichi Uchiyama,[1] Keiichi Edamatsu,[1] and Masaaki Nakayama[2]
[1]*Research Institute of Electrical Communication, Tohoku University, Sendai 980-8577, Japan*
[2]*Department of Applied Physics, Graduate School of Engineering, Osaka City University, Osaka 558-8585, Japan*
(Received 1 April 2016; revised manuscript received 17 August 2016; published 13 September 2016)

We studied the population and coherence dynamics of a biexciton in a planar CuCl microcavity. We developed a time-resolved two-photon polarization spectroscopy technique, by which we extracted the population dynamics of the biexciton even when the biexciton was spectrally overlapped with the lower cavity polariton. The observed lifetime of the cavity biexciton in the weak-coupling regime was much shorter than that of a bare CuCl thin film without a cavity, which directly demonstrates cavity enhancement of the radiative decay rate of the biexciton. The cavity enhancement originates from the hybridization of the unbound two-cavity-polariton state to the biexciton wave function by the biexciton-cavity coupling. By comparing the population and coherence decay curves of the biexciton, we found that the coherence of the cavity biexciton was limited by the radiative population decay.

DOI: 10.1103/PhysRevB.94.115308

Recently, biexcitons (BXs) in semiconductor materials have attracted attention as promising quantum light sources for quantum information technology applications. Entangled photon pair generation has been experimentally demonstrated using the cascade radiation from BXs with a total angular momentum $J = 0$ [1–4]. The generation of squeezed light via BX cascade has also been proposed theoretically [5]. Theoretical works [5–7] have suggested that the use of cavity enhancement in the coupling of BXs and photons is essential in order to improve the photon generation efficiency and the degree of squeezing. In a cavity quantum dot system, a bright source for entangled photon pairs using the BX cascade has already been demonstrated experimentally [4].

In cavity quantum electrodynamics for the exciton-cavity coupled system, there are two regimes, which depend on the magnitude of the exciton-cavity coupling energy $\hbar g_E$, the exciton (EX) dephasing rate $\hbar\gamma_E$, and the cavity photon decay rate $\hbar\gamma_C$. When $\hbar g_E$ is sufficiently larger than both $\hbar\gamma_E$ and $\hbar\gamma_C$, the strong-coupling regime is realized [8]. In the strong-coupling regime, single EXs and single cavity photons are strongly hybridized, forming cavity polaritons. This formation drastically changes the optical spectrum, for example the reflectivity spectrum, around the EX resonance by replacing a single peak with doublet peaks separated by the vacuum Rabi splitting $2\hbar g_E$ [9]. On the other hand, in the weak-coupling regime, i.e., $\hbar g_E \ll \hbar\gamma_E, \hbar\gamma_C$ [8], the optical spectrum is almost the same as a bare sample without a cavity, while the radiative decay rate and efficiency are modified, as a cavity effect [10–12]. For the BX-cavity coupled system, the strong- and weak-coupling regimes are also defined in the same way as for the EX-cavity coupled system. Therefore, similar optical properties are expected, which depend on whether the condition $\hbar g_B \ll \hbar\gamma_B, \hbar\gamma_C$ or $\hbar g_B \gg \hbar\gamma_B, \hbar\gamma_C$ is satisfied, where $\hbar g_B$ denotes the BX-cavity coupling energy and $\hbar\gamma_B$ represents the BX dephasing rate.

At present, there have been few reports on the experimental observation of BXs in a planar cavity. Earlier works have reported the formation of BXs in a cavity by observing the pump-probe (PP) spectrum [13–15]. Recently, the strong- and weak-coupling regimes for BX-cavity coupled systems have been discussed in terms of the change in the four wave mixing (FWM) [16–18] and PP spectra [17,19] as a function of the cavity detuning. For the strong-coupling regime, split peaks arising from the strong hybridization of the BX and cavity photons have been successfully demonstrated [16]. On the other hand, in the case of experiments in the weak-coupling regime [17–19], measured FWM and PP spectra have shown that the BX in a cavity is an almost bare BX, while the temporal FWM response has been much faster than a bare BX [17,18], implying that the BX-cavity coupling strongly enhances the radiative decay rate of the BX in a planar cavity. However, the FWM generally probes the dephasing process, not the radiative decay process. The transient PP signal probing the transition between the cavity polaritons and the BX gives the lifetime of the cavity polaritons [17,19]. Therefore, cavity enhancement in the radiative decay rate for the BX has not yet been observed directly as a change in the lifetime.

In this paper, we report on the lifetime and the dephasing process of a BX in a planar CuCl microcavity. The lifetime was obtained by developing a time-resolved two-photon polarization spectroscopy (TR-TPPS) technique. The original TPPS was developed for studies of the dispersion relations of a polariton and a BX in bulk samples by measuring the transition energy of each state [20]. Here, we have applied the detection scheme of the BX in the TPPS to TR spectroscopy. With the TR-TPPS technique, we separate the optical response originating from the BX-LP transition between the BX and the lower polariton (LP) from that originating from the LP-ground state (LP-G) transition and thus successfully observe the lifetime of the BX. The lifetime and the spectrum observed by the TR-TPPS indicate that the BX in the CuCl microcavity is weakly coupled to the cavity photons through the cavity polaritons. The measurement of a shorter lifetime of the BX in the microcavity as compared to that of a CuCl thin film directly demonstrates the cavity enhancement in the radiative decay rate. Moreover, by directly comparing the decay profiles of the TR-TPPS and the FWM signals, we find that the dephasing rate of the BX in the cavity is limited by the radiative decay rate.

The microcavity in this work was the same CuCl microcavity as in our previous report [18]. The cavity structure consisted of a $\lambda/2$-long Fabry-Perot cavity sandwiched by

*mitumori@riec.tohoku.ac.jp

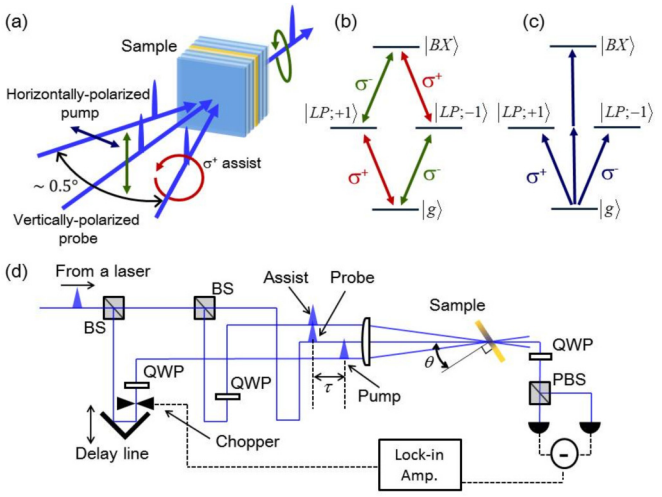

FIG. 1. (a) Illustration of the polarizations of the pump, probe, and assist pulses incident on the sample. (b) Polarization selection rule for a four-level system. $|g\rangle$ and $|\mathrm{BX}\rangle$ represent the ground state and the BX, respectively. $|\mathrm{LP};\pm1\rangle$ are the LP states having orbital angular momenta of ±1. (c) Diagram of the excitation by the pump pulse. The linearly polarized pump pulse excites the BX and populates the $J = \pm1$ LPs equally. (d) Schematic drawing of experimental setup for the TR-TPPS.

distributed Bragg reflector mirrors consisting of eight (ten) pairs of HfO_2/SiO_2 layers for the top (bottom) mirror grown on a sapphire substrate. The quality factor of the cavity was $Q \sim 300$. A 50-nm-thick CuCl active layer was placed at the node of the electric field at the center of the cavity so that we were able to tune the EX-cavity coupling as described below. The angle-resolved reflection spectra at a temperature of 10 K, which can be seen in Ref. [18], showed that the EX-cavity coupling energy for the Z_3 EX was $\hbar g_E = 20$ meV and the cavity detuning $\Delta = E_E - E_C = -88$ meV, where E_E and E_C are the Z_3 EX energy and the photon energy at the cavity resonance for the normal incident angle $\theta = 0^\circ$, respectively. The zero cavity detuning was realized at the incident angle $\theta \sim 24^\circ$. The large negative cavity detuning of the sample at normal incidence allowed us to investigate the cavity detuning effects of the dephasing rate of the BX in the cavity by changing the incident angle of the pump pulses around $\theta \sim 24^\circ$. For more details on the characterization of our CuCl microcavity, see Ref. [18]. Note that the Z_3 exciton corresponds to the split-off-hole exciton and that the Z_3 exciton is the lowest-energy excitonic state in the CuCl crystal [21].

In the TPPS measurement, two beams are used for probing the BX. One beam, referred to as the assist beam, is set to be σ^+ circularly polarized and the other, referred to as the probe beam, is vertically polarized, as illustrated in Fig. 1(a). When the sum of the photon energies of the two beams is resonant with the BX, a transition path from the ground state to the BX exists by absorbing a σ^+ polarized photon from the assist beam and the σ^- component of the vertically polarized probe beam, as shown in Fig. 1(b). Thus, the creation of the BX changes the polarization state of the probe beam passing through the sample [20]. Therefore, in TPPS, the BX is probed by detecting the change in the polarization state of the probe beam. To apply TPPS to TR spectroscopy, we introduced a horizontally polarized pump pulse, as shown in Fig. 1(a). Then, with the time delay τ from the pump pulse, the assist and probe pulses were simultaneously introduced to the sample. The σ^+ and σ^- components in the horizontally polarized pump pulse excite the two LPs with angular momenta $J = \pm1$, as well as the BX, when the LP-G transition is spectrally overlapped with the BX-LP transition, as seen in Fig. 1(c). However, the linearly polarized pump pulse populates both of the LPs equally and they do not contribute to the change in the polarization state of the probe pulse. Therefore, by detecting the pump-induced change in the polarization state of the probe pulse as a function of τ, we can extract the population dynamics of the BX from the pump-induced signals dominated by the LPs in the microcavity.

The TR-TPPS experiment was carried out under the transmission geometry shown in Figs. 1(a) and 1(d). The source of the pump, assist, and probe pulses was the second harmonic light of a femtosecond mode-locked Ti:Sapphire laser. The central photon energy of the incident optical pulses was tuned to 3.186 eV, which corresponds to the two-photon resonant energy of the BX in a CuCl bulk crystal. The bandwidth of the pulses was set to be ~16 meV and the temporal duration was ~100 fs. Figure 1(d) shows the experimental setup for the TR-TPPS measurement. The optical pulse was divided into pump, probe, and assist pulses by two beam splitters (BSs). The polarizations of the pump and probe pulses were horizontal and vertical, respectively. The assist pulse was σ^+ circularly polarized. The pump pulse was chopped by an optical chopper with frequency 200 Hz for the lock-in detection. The three pulses were focused again to the same spot on the sample, which was mounted on a sample holder kept at 3.3 K in a cryostat. Each beam spot had a Gaussian profile with a full width at half maximum (FWHM) of ~100 μm. The three pulses were approximately parallel; the angle between the pulses was set to be as small as 0.5°, as shown in Fig. 1(a). The incident angle θ, i.e., the mean incident angle of the three pulses to the sample normal, was set to be $\theta \sim 27^\circ$. The power density of the pump pulse was set to be ~100 nJ/cm^2/pulse. The intensities of the probe and assist pulses were ~5 and 20 nJ/cm^2/pulse, respectively. The polarization state of the probe pulse was analyzed by measuring the intensity difference of the σ^+ and σ^- components using a quarter-wave plate (QWP), a polarizing beam splitter (PBS), and a balanced photodiode detector. The output signal from the balanced detector was fed into a lock-in amplifier synchronized to the chopping frequency of the pump pulse. Thus, we obtained the TR-TPPS signal as a function of τ. We also observed the TR-TPPS spectra, for which we put a tunable spectral filter consisting of a double-pass (zero-dispersion) diffraction grating after the pulse source. The FWHM of the filtered pulse was estimated to be ~ 2.7 meV. We obtained the TR-TPPS spectra by scanning the photon energy of the filtered pulse while the time delay was fixed to be zero.

The FWM experiment was carried out under a transmission geometry similar to the TR-TPPS experiments. We used the two pulses in the TR-TPPS setup for the excitation. One was the pump pulse with horizontal polarization and wave vector $\mathbf{k}_1$. The other was the probe pulse with wave vector $\mathbf{k}_2$, which was vertically polarized. The intensity of both pulses was set

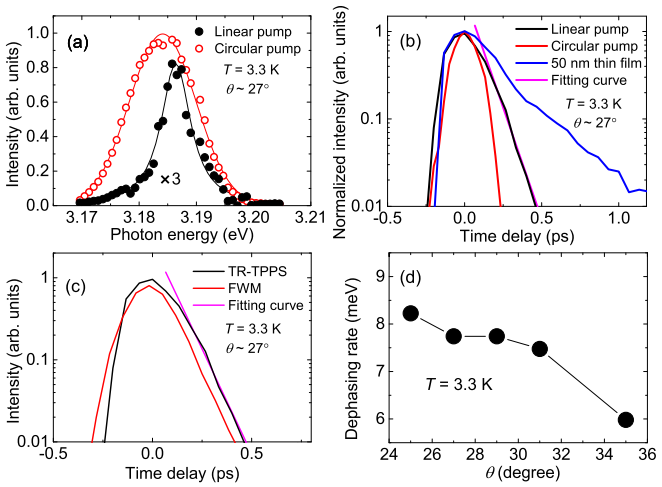

FIG. 2. (a) TR-TPPS spectra for linearly and circularly polarized excitations at zero time delay. (b) Results of TR-TPPS measurements for the linearly and circularly polarized excitations in the microcavity, together with the BX in the 50-nm-thick CuCl film and a fitting curve with a decay time constant of 85 fs. (c) Decay profiles of the TR-TPPS signal for linear excitation and the FWM signal along $2\mathbf{k}_1$-$\mathbf{k}_2$, together with a decay curve with a decay time constant of 85 fs. (d) Dependence of the two-photon dephasing rate $\hbar\gamma_{BG}$ on the incident angle θ.

to ~100 nJ/cm^2/pulse. We detected the FWM signal along $2\mathbf{k}_1$-$\mathbf{k}_2$ as a function of τ.

Figure 2(a) shows the TR-TPPS spectra at zero time delay when the pump pulse was set to be in σ^+ polarization (red open circles) and linear polarization (black circles). For the pump in the circular polarization, the transition to the BX is forbidden, while the $J = 1$ LP is excited. In this case, the TR-TPPS signal is dominated by the pump-induced population difference of the $J = \pm 1$ LPs. Therefore, the TR-TPPS signal in the σ^+ polarized pump originates from the LP and the peak position at 3.184 eV corresponds to the energy position of the LP at the incident angle $\theta \sim 27^\circ$. The TR-TPPS spectrum exhibits a Gaussian-like shape with a FWHM of ~15 meV. This spectral shape is attributed to that of the pump pulse, because the spectral width is close to that of the incident laser pulse (~16 meV) and is slightly narrower than the linewidth of the LP spectrum (~20 meV), which is estimated from the linear reflection spectrum [18].

In contrast, for the linearly polarized pump, the TR-TPPS spectrum drastically changed; it exhibited a shifted peak position (3.186 eV), narrower linewidth, and weaker signal intensity. The linearly polarized pump pulse creates the same amount of $J = \pm 1$ LPs. The equal population of the LPs does not affect the polarization of the probe pulse and has no contribution to the TR-TPPS signal. However, the linearly polarized pump also creates the BX population via two-photon absorption (TPA). As a result, it induces a change in the absorption of the σ^- component in the probe pulse that creates the BX in combination with the σ^+ assist pulse. Thus, the TR-TPPS signal reflects the population change of the BX induced by the linearly polarized pump pulse. Generally, a quantum state created by one-photon absorption is more effectively populated than that of TPA under the same excitation intensity. Therefore, the change in the probe pulse under the linearly polarized excitation for the BX, which is created by TPA, is weaker than that of the circularly polarized excitation for the LP.

According to a theoretical analysis of the original TPPS [20], the TPPS signal is generated by the third-order nonlinear susceptibility $\tilde{\chi}^{(3)}$. Therefore, the measurement of the probe intensity passing through the sample gives $\mathrm{Im}(\tilde{\chi}^{(3)})$, and the spectrum is equivalent to the TPA spectrum. In general, the TPA spectrum around two-photon resonance can be approximated by a Lorentzian function as $\mathrm{Im}(\tilde{\chi}^{(3)}) \propto \mathrm{Im}(\frac{A}{E_{\mathrm{BX}}-2E+i\hbar\gamma_{\mathrm{BG}}})$, where A represents the two-photon transition moment between the BX and the ground state. E_{BX}, E, and $\hbar\gamma_{\mathrm{BG}}$ denote the BX energy, the laser photon energy, and the two-photon dephasing rate of the BX-G transition, respectively. In our experiment, which detects the differential signal caused by the pump pulse, the TR-TPPS spectrum for the linear excitation can be described by the difference of the two Lorentzian spectra with and without the pump pulse. The experimentally observed spectrum exhibits a Lorentzian-like shape, as shown in Fig. 2(a). Therefore, the TR-TPPS signal originates from the pump-induced change in the transition moment A of the BX. The peak position of the spectrum (3.186 eV) represents the two-photon resonant energy of the BX. Therefore, the BX energy in the cavity is estimated to be $E_{\mathrm{BX}} = 6.372$ eV, which is in agreement with the value evaluated in our previous report [18]. We also estimated from the FWHM value of the peak to be $\hbar\gamma_{\mathrm{BG}} \sim 7$ meV. On the other hand, from the FWM experiment in Fig. 2(c), we obtained the two-photon dephasing time of the BX in the cavity as $T_2 \sim 170$ fs, which can be calculated to be $\hbar\gamma_{\mathrm{BG}} \sim 7.7$ meV. The estimated two values agree reasonably with each other. Therefore, the agreements found in the energy position and the linewidth of the BX strongly support the interpretation that TR-TPPS for the linearly polarized excitation successfully probes the BX in the microcavity even when the BX-LP transition is spectrally overlapped with the LP-G transition.

The temporal profiles of the TR-TPPS signal as a function of τ are presented in Fig. 2(b). In the figure, as well as the data for the linearly and circularly polarized pump cases, we plot the result for a bare BX in a 50-nm-thick CuCl film, which is the same as that of the active layer in our microcavity. As mentioned above, the TR-TPPS signal for the circularly polarized pump probes the temporal response of the LP population. The decay profile of the TR-TPPS for the circularly polarized pump was almost the same as the pump pulse profile, indicating the short lifetime of the cavity photons in our low Q cavity, which results in the short lifetime of the LP around the cavity resonance. On the other hand, for the linearly polarized excitation, we observed an exponential decay profile, which arises from the population decay process of the BX in the cavity. We estimated the lifetime T_{1CB} of the BX in the cavity to be $T_{1CB} \sim 85$ fs using a single exponential fit. The value of T_{1CB} gives a radiative decay rate $\hbar\Gamma_{CB} \sim 7.7$ meV. In the thin film without the cavity, we could also observe an exponential decay signal. The decay time constant T_{1BB} of the bare BX was evaluated to be $T_{1BB} \sim 270$ fs with a single exponential fit and gave a radiative decay rate $\hbar\Gamma_{BB} \sim 4.9$ meV. The radiative decay rate of the BX in the cavity is considerably larger than that of the bare BX. This increase in the decay rate and the single peak observed in the TR-TPPS

spectrum in Fig. 2(a) directly indicate that the BX in the cavity is weakly coupled to the cavity photons; the observed increase in the decay rate originates from the cavity enhancement in the radiative decay rate for the BX. We note here that the lifetime $T_{1BB} \sim 270$ fs of the bare BX in the 50-nm thin film is much shorter than the BX lifetime ~30 ps reported for a bulk sample with a thickness of a few μm [22]. We have measured the thickness dependence of the lifetime of the bare BX for samples having thicknesses ranging from 50 to 200 nm. The result shows that the lifetime of the bare BX was almost proportional to the sample thickness. One of the possible reasons for the short lifetime of a BX showing a linear thickness dependence is that the propagation time of the BX between the sample surfaces dominates the lifetime, referred to as the wall collision process, which has been demonstrated in the thickness dependence of the EX lifetime in CuCl thin films [23]. Nevertheless, our important finding here is that the lifetime of the BX in the cavity is considerably shorter than that of the bare BX, indicating the experimental evidence of the cavity enhancement in the radiative decay for the BX.

Figure 2(c) presents the decay profiles of the TR-TPPS for linear excitation and the FWM response in the cavity. The FWM signal was observed along $2\mathbf{k}_1$-$\mathbf{k}_2$, where the signal decay time in the positive τ regime gives the two-photon dephasing time T_2 of the BX. The decay time constants of the TR-TPPS and the FWM signals coincide with each other, indicating that the dephasing time reaches the radiation limit $T_2 = 2T_{1CB}$ ($T_2 \sim 170$ fs) because twice the decay time of the FWM signal gives the dephasing time. The radiation limit of the dephasing time suggests that the radiative process plays a major role in the dephasing process and other effects, such as phonon scattering, do not contribute to the dephasing process.

In cavity systems, it is well known that a high Q cavity with a small mode volume V for the cavity photon enhances the radiative decay rate of a quantum state, referred to as the Purcell effect [24]. In planar cavities for the EX systems, theoretical works have pointed out that the radiative decay rate in an ideal cavity is a few times larger than that of a bare sample [12]. On the other hand, in a realistic cavity, the rate is expected to be smaller than that of a bare EX. In particular, for a $\lambda/2$ node cavity, the rate is predicted to be extremely small [11]. In our experiment, we found that the decay process of the BX in the cavity was governed by the radiative decay enhanced by the BX-cavity coupling, although our cavity was a $\lambda/2$ node cavity with low Q. Therefore, our experimental findings suggest that the physical mechanism of the cavity effect of the BX in a cavity is different from that of the EX-cavity coupled system and thus also that of the Purcell effect.

For the BX-cavity coupled system, recent theoretical studies have treated a cavity BX as a two-particle state [5,7,25]. In those, the wave function of the cavity BX is described as $|CB\rangle = a_{BB}|BB\rangle + a_{XX}|XX\rangle + a_{XC}|XC\rangle + a_{CC}|CC\rangle$, using a superposition of the bare BX $|BB\rangle$, the unbound two-exciton state $|XX\rangle$, the one-exciton-one-cavity-photon state $|XC\rangle$, and the two-cavity-photon state $|CC\rangle$. Here, we neglect the spin degree of freedom for simplicity, and a_i denotes the probability amplitude of a state $|i\rangle$. When the EX-cavity coupled system is in the strong-coupling regime, the cavity BX is renormalized as $|CB\rangle = a_{BB}|BB\rangle + a_{PP}|PP\rangle$, where $|PP\rangle$ represents the unbound two-cavity-polariton state [5,7,25]. Therefore, the BX-cavity coupling gives the hybridization of the two-cavity-polariton state to the cavity BX wave function. This means that the BX in a cavity is coupled to the cavity photons indirectly through the cavity polaritons, and indicates that the two-cavity-polariton state strongly affects the lifetime of the BX in a cavity.

In our cavity, the EX-photon coupling energy for the Z_3 EX is $\hbar g_E = 20$ meV, which is close to the bare-BX binding energy $\Delta E_{\mathrm{BX}} = 32$ meV. This energy relation gives a condition of $E_{\mathrm{BX}} \sim 2E_{\mathrm{LP}}$ around zero detuning. Therefore, we infer that the two-cavity-polariton state hybridizing to the BX in our cavity is mainly composed of the unbound two-LP state. As shown in Fig. 2(b), the LP in our cavity exhibits an extremely short lifetime, suggesting that the two-cavity-polariton state also shows an extremely fast decay, which results in the shorter lifetime of the BX in the cavity than the bare BX. Consequently, the radiative decay rate of the BX in the cavity is larger than that of the bare sample. In addition, recently, theoretical calculations have shown that entangled photon pairs are most efficiently generated with a condition of $E_{\mathrm{BX}} \sim 2E_{\mathrm{LP}}$, when the BX cascade in a planar cavity is used for the generation [6,7]. Thus, we guess that the energy relation in our cavity also contributes to the successful enhancement in the radiative decay rate of the BX.

Finally, we briefly comment on the incident angle θ dependence of the two-photon dephasing rate $\hbar\gamma_{\mathrm{BG}}$ of the BX in the cavity obtained by the FWM measurement. The data are plotted in Fig. 2(d). The dependence of $\hbar\gamma_{\mathrm{BG}}$ is equivalent to that of the radiative decay rate $\hbar\Gamma_{CB}$ of the BX on θ when we assume $\hbar\gamma_{\mathrm{BG}} = \hbar\Gamma_{CB}$ ($T_2 = 2T_{1CB}$). Figure 2(d) shows that $\hbar\gamma_{\mathrm{BG}}$ slightly decreases with increasing θ. In the EX-cavity coupled system, larger θ generally gives larger positive detuning [26], which increases the composition of the EXs in the LP, and yields the LP a slower population decay time [27]. As mentioned above, in our cavity, the population decay of the LP affects the BX lifetime through the BX-cavity coupling. Therefore, the observed dependence on θ originates from the change in the radiative decay of the LP, which hybridizes to the BX as the two-LP state by the BX-cavity coupling.

In conclusion, we developed a time-resolved two-photon polarization spectroscopy technique for estimating the lifetime of a BX in a microcavity. Using this technique, we successfully observed the BX even when the BX-LP transition was overlapped with the LP-G transition, which shows that the developed technique is a powerful tool for studying the BX population dynamics. The observed lifetime of the BX in the cavity was much shorter than that of the bare BX in the thin film, which demonstrated the cavity enhancement in the radiative decay rate for the BX-cavity coupled system, suggesting that the BX is coupled with the cavity photons through the LPs. We found that the dephasing process of the BX in the cavity was solely governed by the radiation limit. The BX-cavity coupled system will be useful for developing high efficiency quantum light sources based on semiconductors.

The authors are grateful to K. Miyazaki and D. Kim of Osaka City University for their help in sample preparation. They also thank H. Ajilki of Tokyo Denki University, H.

Ishihara of Osaka Prefecture University, and M. Sadgrove of Tohoku University for helpful discussions. This work was supported by a Grant-in-Aid for Scientific Research (Grants No. 15H03678 and No. 22244035) and a Grant-in-Aid for Challenging Exploratory Research (Grant No. 24654081) from Japan Society for the Promotion of Science.

[1] K. Edamatsu, G. Oohata, R. Shimizu, and T. Itoh, Nature (London) **431**, 167 (2004).
[2] G. Oohata, R. Shimizu, and K. Edamatsu, Phys. Rev. Lett. **98**, 140503 (2007).
[3] C. L. Salter, R. M. Stevenson, I. Farrer, C. A. Nicoll, D. A. Ritchie, and A. J. Shields, Nature (London) **465**, 594 (2010).
[4] A. Dousse, J. Suffczyński, A. Beveratos, O. Krebs, A. Lemaître, I. Sagnes, J. Bloch, P. Voisin, and P. Senellart, Nature (London) **466**, 217 (2010).
[5] H. Oka and H. Ajiki, Phys. Rev. B **83**, 045305 (2011).
[6] H. Ajiki and H. Ishihara, J. Phys. Soc. Jpn. **76**, 053401 (2007).
[7] H. Oka and H. Ishihara, Phys. Rev. Lett. **100**, 170505 (2008).
[8] V. Savona, L. C. Andreani, P. Schwendimann, and A. Quattropani, Solid State Commun. **93**, 733 (1995).
[9] C. Weisbuch, M. Nishioka, A. Ishikawa, and Y. Arakawa, Phys. Rev. Lett. **69**, 3314 (1992).
[10] T. Yamauchi, Y. Arakawa, and M. Nishioka, Appl. Phys. Lett. **58**, 2339 (1991).
[11] G. Björk, S. Machida, Y. Yamamoto, and K. Igeta, Phys. Rev. A **44**, 669 (1991).
[12] G. Björk, S. Machida, and Y. Yamamoto, in *Confined Electrons and Photons*, edited by E. Burstein and C. Weisbuch (Plenum, New York, 1995).
[13] X. Fan, H. Wang, H. Q. Hou, and B. E. Hammons, Phys. Rev. B **57**, R9451 (1998).
[14] U. Neukirch, S. R. Bolton, N. A. Fromer, L. J. Sham, and D. S. Chemla, Phys. Rev. Lett. **84**, 2215 (2000).
[15] M. Saba, F. Quochi, C. Ciuti, U. Oesterle, J. L. Staehli, B. Deveaud, G. Bongiovanni, and A. Mura, Phys. Rev. Lett. **85**, 385 (2000).
[16] T. Baars, G. Dasbach, M. Bayer, and A. Forchel, Phys. Rev. B **63**, 165311 (2001).
[17] P. Borri, W. Langbein, U. Woggon, A. Esser, J. R. Jensen, and J. M. Hvam, Semicond. Sci. Technol. **18**, S351 (2003).
[18] S. Matsuura, Y. Mitsumori, H. Kosaka, K. Edamatsu, K. Miyazaki, D. Kim, M. Nakayama, G. Oohata, H. Oka, H. Ajiki, and H. Ishihara, Phys. Rev. B **89**, 035317 (2014).
[19] P. Borri, W. Langbein, U. Woggon, J. R. Jensen, and J. M. Hvam, Phys. Rev. B **62**, R7763 (2000).
[20] M. Kuwata, J. Phys. Soc. Jpn. **53**, 4456 (1984).
[21] A. Goldmann, Phys. Status Solidi B **81**, 9 (1977); H. Overhof, *ibid.* **97**, 267 (1980).
[22] H. Akiyama, M. Kuwata, T. Kuga, and M. Matsuoka, Phys. Rev. B **39**, 12973 (1989).
[23] D. K. Shuh, R. S. Williams, Y. Segawa, J. I. Kusano, Y. Aoyagi, and S. Namba, Phys. Rev. B **44**, 5827 (1991).
[24] E. M. Purcell, Phys. Rev. **69**, 37 (1946).
[25] H. Oka, K. Taniguchi, H. Ajiki, and H. Ishihara, Phys. Rev. B **78**, 245420 (2008).
[26] R. Houdré, C. Weisbuch, R. P. Stanley, U. Oesterle, P. Pellandini, and M. Ilegems, Phys. Rev. Lett. **73**, 2043 (1994); G. Oohata, T. Nishioka, D. Kim, H. Ishihara, and M. Nakayama, Phys. Rev. B **78**, 233304 (2008).
[27] B. Sermage, S. Long, I. Abram, J. Y. Marzin, J. Bloch, R. Planel, and V. Thierry-Mieg, Phys. Rev. B **53**, 16516 (1996); X. Marie, P. Renucci, S. Dubourg, T. Amand, P. Le Jeune, J. Barrau, J. Bloch, and R. Planel, *ibid.* **59**, R2494 (1999).